Model-independent wavefront aberration measurement of multi-surface optical systems

Lei Liu[1], Hongshun Zhang[1], Xianlei Liu[1] and Xiaodong Zhang[1,#]

1 State Key Laboratory of Precision Measuring Technology & Instruments, Laboratory of Micronano Manufacturing Technology, Tianjin University, Tianjin 300072, China
Corresponding Author / Email: Zhangxd@tju.edu.cn

KEYWORDS: Wavefront aberration, Multi-surface optical systems, Phase deflectometry

Wavefront aberration is commonly used to evaluate the performance of optical systems. The phase-assisted wavefront aberration measurement method has been widely applied due to its high precision and strong resistance to environmental disturbances. However, current research on this method generally requires known models of optical systems under test to achieve wavefront reconstruction and system error correction. In this paper, a phase-assisted method with moving screen process is designed to calculate the direction of light rays and complete wavefront reconstruction. Additionally, error correction algorithms are proposed for both focused and afocal optical systems under test. These improvements do not rely on system models, which greatly expands the applicability of the phase-assisted wavefront aberration measurement method. This paper conducts measurements on a focused three-surface optical system and an afocal two-surface optical system, comparing the results with those obtained from the interferometer.

NOMENCLATURE

W = wavefront
$P_1(x_1, y_1, z_1)$ = screen pixel at Position 1
$P_2(x_2, y_2, z_2)$ = screen pixel at Position 2
I_1, I_2, I_3, I_4 = images of the measured system captured by the camera during four-step phase shifting
I = aperture region
n = number of points on the edge of aperture region
r = radius of points on the edge of aperture region
$\overline{r}$ = mean radius of points on the edge of aperture region
ϕ = radius consistency of effective aperture region

1. Introduction

Wavefront aberration, as a comprehensive evaluation metric for optical system performance, can be used to analyze various indicators such as the point spread function, spherical aberration, and astigmatism [1]. It plays a crucial role in assessing the design and manufacturing quality of optical systems.

The phase-assisted wavefront aberration measurement method is an emerging approach for wavefront aberration measurement. Compared to interferometry, it exhibits strong resistance to environmental disturbances and achieves comparable accuracy when measuring wavefront aberrations on the order of sub-microns and above [2]. This method also has advantages over the Shack-Hartmann method, including a simpler structure and higher resolution. The key to the phase-assisted wavefront aberration measurement method lies in determining the direction of actual and ideal rays. Existing studies generally require knowledge of the surface shape and pose parameters of the measured optical system to obtain a reference wavefront under ideal conditions. This method typically employs reverse Hartmann optical path in combination with ray simulation, so the primary factors affecting accuracy are the relative position and orientation deviations between the components in the measurement system and the optical system under test. Gong et al. focused their research on enhancing accuracy by analyzing the relative position errors of the optical system under test through ray tracing and eliminating their impact on the measurement results with optimization [3]. However, this optimization still requires knowledge of all key parameters of the devices and the optical system under test. Jiang et al. introduced a pre-measurement alignment method using markers displayed on a screen to assist in aligning the optical system under test, but this approach can only correct for misalignment of the device centers and cannot address issues such as defocus and tilt [4]. The requirement of knowing the parameters of the optical system under test significantly limits the applicability of the wavefront aberration measurement method based on phase deflectometry. Besides, due to the complexity of light propagation and the difficulty in aligning the field of view in multi-surface optical systems, current research on phase-assisted wavefront aberration measurement generally focuses only on individual optical components [5].

To address this issue, we propose a model-independent wavefront

aberration measurement method for multi-surface optical systems. We have designed specific measurement setups for both focused and afocal optical systems and developed a high-precision optical alignment strategy to correct the impact of the test object's pose on measurement results. Through simulations, we addressed the focusing process during the measurement of focused systems using a phase-assisted focus alignment method, and we tackled the aperture alignment problem in afocal systems by evaluating radius consistency. These alignment strategies do not rely on the parameters of the optical system under test, ensuring high flexibility and applicability while maintaining accuracy.

2. Phase-assisted wavefront aberration measurements of multi-surface optical systems

2.1 Measurement principle

The phase-assisted wavefront aberration measurement scheme is illustrated in the figure below. To better match the optical path of the system under test, an external pinhole aperture and a telecentric lens are placed in front of the camera for focused and afocal optical paths, respectively. This measurement method fundamentally reconstructs the wavefront W by determining the ray direction vectors, making the key challenge the accurate determination of these vectors. We address this challenge using the screen-shifting method. As shown in Fig. 1, the industrial screen sequentially displays sinusoidal grayscale patterns with horizontal and vertical stripes through multi-step phase shifting at each position. After phase retrieval via the multi-step phase-shifting method, phase unwrapping is performed spatially. Each pixel on the screen is then uniquely identifiable through its encoded horizontal and vertical phase information. The camera captures the images of these patterns as they are projected through the multi-surface optical system under test. The phase information from these images is then decoded to establish the mapping relationship between each pixel on the camera's CCD and the corresponding pixel on the screen.

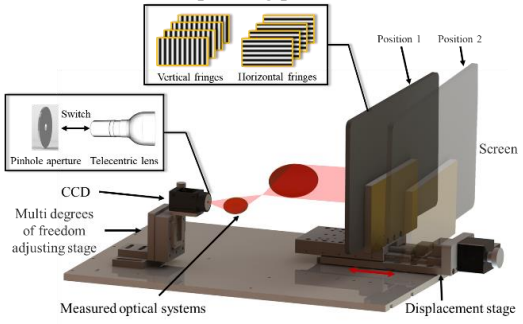

Fig. 1 Scheme of measurement principle.

The ray formed by connecting points P_1 and P_2 in physical space can represent the direction vector of the light ray. The partial derivatives of the wavefront W along the two orthogonal dimensions can be expressed as:

$$\frac{\partial W}{\partial x}=\frac{x_2-x_1}{\sqrt{(x_2-x_1)^2+(y_2-y_1)^2+(z_2-z_1)^2}} \tag{1}$$

$$\frac{\partial W}{\partial y}=\frac{y_2-y_1}{\sqrt{(x_2-x_1)^2+(y_2-y_1)^2+(z_2-z_1)^2}} \tag{2}$$

2.2 Phase-assisted focus alignment for focused systems

By using a pinhole instead of a standard industrial lens, the measurement setup not only ensures that only a single field of view is measured but also avoids the impact of lens aberrations on the final wavefront aberration results. However, the relative pose errors of the measurement setup can still influence the measurement outcomes. The main sources of error include screen tilt (ST), screen motion direction error (SMDE), defocus error (DE) and lateral misalignment (LM) of the system under test. Since the tilt error of the system under test can be identified by evaluating radius consistency—a method to be introduced in Section 2.3—this tilt error is not simulated in this analysis. As shown in Fig. 2, defocus error has a particularly significant impact on the measurement results. Defocus increases the magnitude of aberrations without altering the distribution of wavefront aberration, making it difficult to accurately subtract its effect even with optimization and correction.

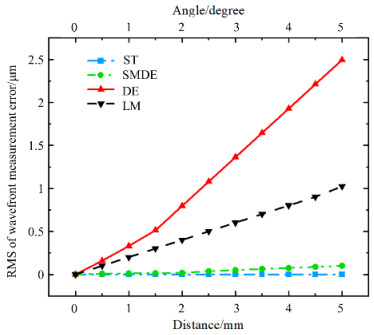

Fig. 2 Influence simulation of main errors.

In addition to the conventional optical alignment process, a phase-assisted method for focus alignment is proposed for addressing defocus errors. When the pinhole is positioned in front of the focal point, the angle of inclination between the light rays traced backward from the pinhole and the optical axis increases. After reflection from the optical system under test, these rays tend to diverge in the object space. Conversely, when the aperture is placed behind the focal point, the inclination angle decreases, causing the reflected rays to converge. Only when the aperture is at the focal point do the rays approach a parallel emission trend.

Four-step phase-shifted horizontal and vertical fringe patterns are displayed at two positions of the screen, and the camera captures images of these patterns after they pass through the test optical system, followed by phase retrieval and unwrapping. To enhance efficiency, four pixel coordinates are extracted symmetrically around the center from the phase map at Position 1 and recorded along with their corresponding phases. In the phase map at Position 2, the coordinates of four pixels are then searched based on the previously recorded phases. As shown in Fig. 3, the movement of these four pixel points' is determined according to the phase correspondence.

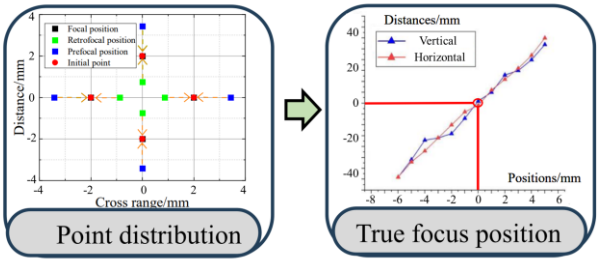

Fig. 3 Principle of phase-assisted focus alignment.

As shown in the Fig. 3, the relationship curve between defocus amount and pixel displacement is approximately linear. Therefore, by

taking a series of measurements along the optical axis near the focal point, this method can be used to assess pixel displacement and determine the focal point position through linear fitting. The phase-assisted focusing algorithm enables precise quantification of defocus, offering greater accuracy compared to traditional laser-assisted focusing methods. Furthermore, it avoids the over-optimization issues that may arise when errors are removed from final wavefront aberration measurements.

As shown in Fig. 4, the proposed phase-assisted focus alignment is applied to a focused optical system composed of three freeform mirrors. The measurement is performed using a sixteen-step phase shifting method. The RMS of the wavefront aberration measured with our method is 0.357 μm, while the interferometer measurement yields an RMS of 0.302 μm. The error distributions between the two measurements are generally consistent.

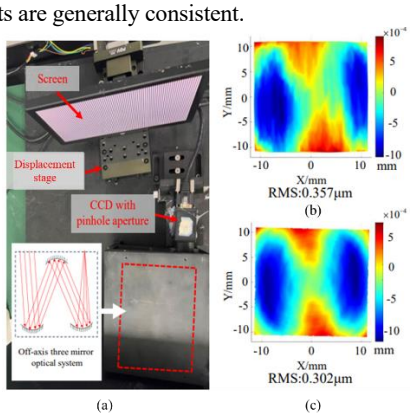

Fig. 4 Measurement of a three-surface optical system. (a) Experiment setup, (b) Result of our method, (c) Result of a Zygo interferometer.

2.3 Tilt error correction algorithm for afocal systems

A telecentric lens is employed to constrain the field of view angle when measuring afocal optical systems, thereby reducing influence from other fields. Because focal alignment is not required, the primary sources of error are screen tilt (ST), screen motion direction error (SMDE), lateral misalignment (LM) and tilt (T) of the test optical system. As shown in Fig. 5, the relationship curves between these errors and the RMS of wavefront aberration are simulated. The motion direction of the screen is determined by the displacement stage, and alignment of the displacement stage with the camera's optical axis can be assisted with a point laser. Tilt error of the test optical systems results in measurements of additional fields of view. The impact of this error depending on the consistency of aberrations between different fields of view in the optical systems under test.

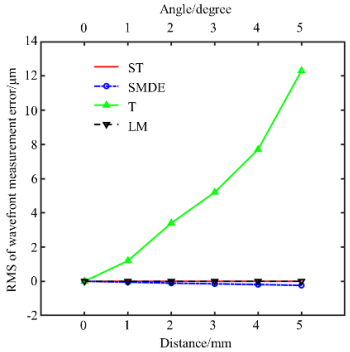

Fig. 5 Influence simulation of main errors.

Since the optical system's nominal field aperture is generally circular in profile, a tilt error correction method based on radius consistency is designed. This method involves displaying images on the screen. The edges of many optical components, particularly mirrors, are machined with chamfers. When only a plain white image is displayed, it is challenging to distinguish between the chamfered areas and the effective mirror surface in the images captured by the camera due to the lack of gray-level contrast. To address this, four-step phase-shifted fringe patterns are displayed on the screen, and by capturing the images of these fringe patterns through the optical system under test, the effective aperture area I can be calculated.

$$I = \{I_t > 1 \mid I_t = \frac{1}{4}\sum_{i=1}^{4}|I_i - I_m|\} \tag{3}$$

Where, the intermediate variable I_m is defined as:

$$I_m = \frac{1}{4}\sum_{i=1}^{4} I_i \tag{4}$$

The radius consistency ϕ can be calculated as below, and the lower ϕ is, the closer the aperture is to a perfect circle.

$$\phi = \frac{\sum_{i=1}^{n}|r_i - \bar{r}|}{n} \tag{5}$$

A simulation is conducted to generate the range of radius consistency variation for a two-surface optical system with off-axis parabolic mirrors when tilted within the range of -4 to +5°. As shown in Fig. 6, a -1° tilt results in a deviation of 20 pixels. By further extracting the region I with sub-pixel precision and evaluating radius consistency using this phase-shifting method, the tilt angle of the test optical system can be constrained within a specific range. This approach can calibrate the tilt of the test afocal system with only the measurement setup itself, rather than other high-precision instruments.

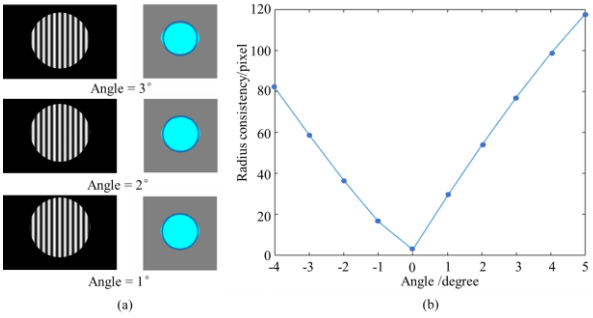

Fig. 6 Simulation of radius consistency variation. (a) Images when angle vary from 1 to 3°, (b) Curve of radius consistency with angle.

As illustrated in Fig. 7, the proposed tilt correction algorithm is applied to measure the wavefront aberration of a afocal optical system composed of two off-axis parabolic mirrors. The measurement is also performed using a sixteen-step phase-shifting method. The RMS of the wavefront aberration obtained with our method is 0.499 μm, while the interferometer measurement yields an RMS of 0.457 μm. The error distributions between the two measurements are generally consistent.

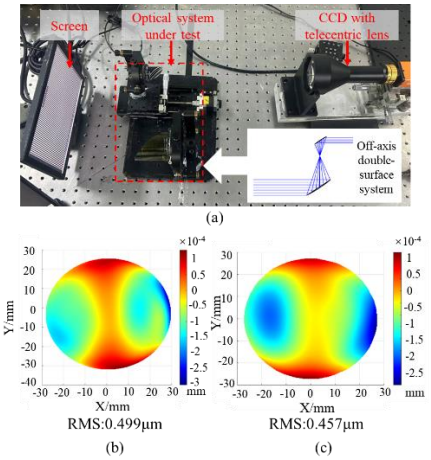

Fig. 7 Measurement of a double-surface optical system. (a) Experiment setup, (b) Result of our method, (c) Result of a Zygo interferometer.

3. Conclusions

This paper presents improvements to the traditional phase-assisted wavefront aberration measurement method. For both focused and afocal optical systems under test, we designed corresponding focus alignment and tilt correction algorithms to address the posture error of test optical systems, which most significantly impact measurement accuracy. These correction algorithms do not require prior knowledge of the key parameters of the optical system being measured, making it highly versatile and capable of accurately measuring the wavefront aberrations of multi-surface optical systems with unknown models.

ACKNOWLEDGEMENT

We thank our colleagues for the many hours of stimulating technical discussions revolving around this and other research. This research is supported by National Natural Science Foundation of China (NSFC) (No. 52105476), Technology Innovation Guidance Project (Fund) of Tianjin (No. 23YDTPJC00640).

REFERENCES

1. Restrepo J, Stoerck P J, Ihrke I. "Ray and wave aberrations revisited: a Huygens-like construction yields exact relations." JOSA A, Vol. 33, No. 2, pp. 160-171, 2016.
2. Su P, Parks R E, Wang L, et al. "Software configurable optical test system: a computerized reverse Hartmann test." Applied optics, Vol. 49, No. 23, pp. 4404-4412, 2010.
3. Gong Z, Wang D, Xu P, et al. "Geometrical error calibration in reflective surface testing based on reverse Hartmann test." Applied Optical Metrology II., Vol. 10373, pp. 133-141, 2017.
4. Jiang L, Zhang X, Fang F, et al. "Wavefront aberration metrology based on transmitted fringe deflectometry." Applied Optics, Vol. 56, No. 26, pp. 7396-7403, 2017.
5. Wang D, Xu P, Gong Z, et al. "Transmitted wavefront testing with large dynamic range based on computer-aided deflectometry." Journal of Optics, Vol. 20, No. 6, pp. 065705, 2018.